ELSEVIER

Chemical Engineering Journal 137 (2008) 471–479

Chemical Engineering Journal

www.elsevier.com/locate/cej

Experimental and modeling of fixed-bed reactor for yellow phosphorous tail gas purification over impregnated activated carbon

Liping Ma *, Ping Ning, Yuanyuan Zhang, XueQian Wang

Faculty of Environment Science and Engineering, Kunming University of Science and Technology, Kunming, Yunnan 650093, PR China

Received 15 January 2007; received in revised form 7 April 2007; accepted 22 April 2007

Abstract

When yellow phosphorous tail gas will be used as chemical raw material gas to produce high accessional products such as formate, oxalate, methanol and so on, pretreatment process by its purifying could limit its application. In this paper, two kinds of impregnated activated carbon catalysts and catalytic oxidation reaction for purifying H_2S and PH_3 contained in tail gas have been studied in laboratory-scale and pilot-plant fixed-bed reactor. The concentration of both H_2S and PH_3 could be less than 10 mg/m^3 over these two kinds of catalysts. Reaction kinetics for the catalytic oxidation of H_2S and PH_3 over the mixed catalyst has also been studied on differential reactor, and kinetic model for both compounds have been formulated, which are subsequently implemented in the modeling of the pilot-plant fixed-bed reactor. A two-dimensional un-steady reaction model which includes both physical adsorption and catalytic reaction process was developed for binary gas mixture purification in fixed-bed. Results from model calculation are reasonably well agreement with the experimental data. It is helpful for a thorough explanation of the observed pilot-plant reactor performance and designing in industrial process.
© 2007 Elsevier B.V. All rights reserved.

Keywords: Yellow phosphorous tail gas; Catalytic oxidation; Impregnated activated carbon; Fixed bed; Modeling

1. Introduction

Yellow phosphorous is the main source for phosphorous chemical engineering. During the producing of yellow phosphorous by electric furnace method, about 2500–3000 m^3 tail gas will be let out when 1 t yellow phosphorous was produced, which is one of the main sources for air pollution in most cities in PR China [1]. The main contain of yellow phosphorous tail gas is about 85–95% carbon monoxide, which cause damage for environment and a huge waste of CO when it is exhaust into atmosphere. Since 1980's, C_1 chemistry had got a great development especially in CO synthesizing technology. Many products such as methylformiate, dimethylether, ethanoic acid, methanol and methyl carbonate can be synthesized from CO. If yellow phosphorous tail gas can be used as raw material gas to synthesize chemically product, it cannot only avoid environmental pollution but also reduce the cost of yellow phosphorous production. However, by now only 20–25% yellow phosphorous tail gas has been used as fuel and the rest is let out into the air, few of them is used to produce some cheap products such as trimeric sodium phosphate, etc. [2]. The main reason to restrict wildly use of yellow phosphorous tail gas is that it contains phosphorous (PH_3, P_4), sulfur (H_2S), which can stark influence the reaction of carbonyl combination even at very low concentration. The heat value of tail gas is about 10,000 kJ/m^3. How to multipurpose use yellow phosphorous tail gas is one of the valuable things. It must obtain high purity CO when it is used as chemical raw material. Therefore, yellow phosphorous tail gas must be pretreated before it is used.

For the purposes of further products of yellow phosphorous tail gas, purifying technology have been researched for many years such as: washing with water to get rid of fly ash, SiF_4 and part of H_2S and HF; washing with water and sodium (NaOH 10–15%); purifying with the method of TSA-PSA [3,4], etc. For some high quality required of CO, deep desulfurization and dephosphorous (both sulfur and phosphorous contained less than 1 ppm) technologies are needed.

During the past several decades, most researches were focus on removing H_2S by adsorption and catalytic oxidation methods. Westmoreland and Harrison [5] researched that some metal oxide such as Fe, Zn, Mo, Mn, Sr, B, Co, Cu and W have better capacity for H_2S removal. Many works were focus on H_2S

* Corresponding author. Tel.: +86 871 5170905; fax: +86 871 5170906.
E-mail address: lipingma22@hotmail.com (L. Ma).

1385-8947/$ – see front matter © 2007 Elsevier B.V. All rights reserved.
doi:10.1016/j.cej.2007.04.032

Nomenclature

b_i	Langmuir constant of i
c_i	i concentration in gas phase (kg/m^3)
c_i^*	i concentration at equilibrium (kg/m^3)
d	diameter of fixed bed (m)
D_{zi}	axial diffusion constant of i
D_{ri}	radius diffusion constant of i
k	reaction rate constant of PH_3 (1/min)
k_1	reaction rate constant of H_2S (kg/s Pa)
k_2	reaction rate constant of H_2S (1/Pa)
K	adsorption mass transfer constant (m^3/kg s)
Q_{mi}	monolayer maximum adsorption amount (kg/kg)
r	radius of fixed bed (m)
R_i	reaction rate of i (kg/s m^3)
S_{cat}	catalytic surface area per unit catalyst volume (m^2/m^3)
t	time (s)
u	flow velocity (m/s)
W_S	amount of S loading on catalyst (kg/kg)
X_i	i loading in activated carbon (kg/kg)
z	length of fixed bed (m)

Greek letters

ε	viodage of fixed bed
ρ_c	density of activated carbon (kg/m^3)

Superscript

*	at equilibrium

Subscript

i	compound index of gas

removal from coal gas by limestone adsorbents [6–10]. However, less report had been found about PH_3 removal from gas phase except chemical vapor deposition [11,12]. Among various methods for H_2S and PH_3 removal reported in the literature, catalytic oxidation at low temperature is less reported [13–16]. To our knowledge, there is no systematic study of binary mixture gas purification contained both H_2S and PH_3 at very low concentration, and this is the sticking point for yellow phosphorous tail gas purification.

In the previously work of our group, it has been found that activated carbon impregnated with metal and other solution has better adsorption capacity for sulfur and phosphorous removing from tail gas. During this process, catalytic oxidation reaction for H_2S and PH_3 take place over impregnated activated carbon. Therefore, it can be assumed that physical adsorption and catalytic oxidation reaction occur simultaneously. In the present work, adsorption isotherm, dynamic behavior and chemical kinetics have been studied over impregnated activated carbon for desulfurization and dephosphorous. The influences of operating variables on catalytic oxidation in both laboratory-scale and pilot-plant fixed bed were investigated. For the purpose of optimal designing of gas–solid reactor and seeking for the optimal operation condition, a simulation model also has been given for predicting the process of both physics adsorption and chemical reaction for mixture gas in fixed-bed reactor.

2. Mechanism

The mechanism of removing H_2S has been studied including adsorption-clause process, liquid redox process and direct oxidation at lower temperature in presence of a catalyst [17,18]. Highly removal efficient and high sulfur capacity up to 60% (g/g cat.) are obtained by catalytic oxidation over impregnated activated carbon [19]. Whereas less study has been found about the removal of PH_3 from mixed gases.

The prior investigation for catalytic reaction on activated carbon was

$$H_2S\,(g) + \tfrac{1}{2}O_2 \rightarrow H_2O\,(g) + S\,(s).$$

Elemental sulfur formed in the oxidation is deposited on carbon catalyst which causes the continuous change in effectiveness factor due to the texture of catalyst changing as a result of sulfur deposition and gradual decrease in the number of active sites due to their physical covering by sulfur [20]. The amount of sulfur formed on is plotted against the reciprocal of time to processing the data. For removal of H_2S in yellow phosphorous tail gas over impregnated activated carbon, catalytic oxidation reaction takes place at the existing of O_2. At the same time, reactions may take place simultaneously for P_4 and PH_3 existed in tail gas, which will be analyzed below.

An ample amount of O_2 contained in tail gas could be used in these catalyst oxidation reactions. Previous work in our group had shown that in addition to oxidation-reductive reaction of impregnated activated carbon bed, there were some H_2S and PH_3 reduction in tail gas through the carbon bed at different temperature. Therefore, it can be assumed that physical adsorption and catalytic oxidation reaction occur simultaneously over the impregnated activated carbon.

2.1. Equilibrium adsorption of gas mixture

Except H_2S and PH_3, yellow phosphorous tail gas contains about 85–90% CO, 2–5% N_2, 1–8% H_2O, 1–4% CO_2, O.5% H_2 and 0.3% CH_4 and 0.5% O_2. The measurement of mix-gas adsorption is certainly tedious. However, models or correlation for mixed-gas adsorption should be capable of predicting from pure gas isotherms. Langmuir isotherm for single-gas adsorption can readily be extended to an n-component mixture [21]. The Langmuir equation for single component is:

$$X = \frac{Q_m b y}{1 + by} \tag{1}$$

When adsorption for a mixture gas, supposing each species maintains its own molecular area, and the area covered by one molecule that is not influenced by the presence of other species on the surface as in single-gas adsorption, the amount adsorbed for i in the mixture is:

$$X_i = \frac{Q_{mi} b_i c_i}{1 + \sum_i^n b_i c_i} \tag{2}$$

For the adsorption of tail gas, taking H_2S and PH_3 as an representation for sulfur and phosphorous components and only these two components are adsorbed on carbon, the rest compounds in tail gas were considered as an inert gas which cannot be adsorbed on adsorbent, therefore Eq. (2) would be calculated for binary mixture gas for H_2S and PH_3 ($n=2$).

2.2. Chemical reaction kinetic of H_2S and PH_3

During the physical adsorption process for H_2S and PH_3, catalytic oxidation reaction take place under the existing of oxygen contained in tail gas over impregnated activated carbon. The mechanisms associated with oxidation process are summarized as follow:

$$P_4 + 3O_2 \xrightarrow{\text{cat.}} 2P_2O_3 \quad \text{(R1)}$$

$$P_4 + 5O_2 \xrightarrow{\text{cat.}} 2P_2O_5 \quad \text{(R2)}$$

$$2PH_3 + 3O_2 \xrightarrow{\text{cat.}} P_2O_3 + 3H_2O \quad \text{(R3)}$$

$$PH_3 + 2O_2 \xrightarrow{\text{cat.}} H_3PO_4 \quad \text{(R4)}$$

$$2H_2S + O_2 \xrightarrow{\text{cat.}} 2S + 2H_2O \quad \text{(R5)}$$

P_4 and PH_3 were oxide into P_2O_3 and P_2O_5 in fixed bed. The adsorptive capacity for P_2O_3 and P_2O_5 is far more than that for P_4 and PH_3, therefore P_2O_3 and P_2O_5 were adsorbed on the impregnated activated carbon. S was adsorbed on the impregnated activated carbon finally as a oxidation product of H_2S, here the impregnated activated carbon take the role of adsorbent and catalyst. Catalyst out of service can be regenerated.

Kinetic mechanism for H_2S oxidation can be summarized as four steps: diffusion–dissolution–adsorption-reaction. When tail gas goes into the reactor, part of aqueous contained in the gas was adsorbed on activated carbon and became a thin membrane. H_2S and O_2 molecules diffused into the pore of solid particle and solved in the aqueous membrane and then deposited. This mechanism, listed below, consists of eight independent forward pathways for oxidation of H_2S, and their corresponding kinetic rate expressions.

$$H_2S\,(g) \overset{K_{AH}}{\longleftrightarrow} H_2S\,(l) \quad \text{(i)}$$

$$O_2\,(g) \overset{K_{BH}}{\longleftrightarrow} O_2\,(l) \quad \text{(ii)}$$

$$H_2S\,(l) \overset{K_{e1}}{\longleftrightarrow} H^+ + HS^- \quad \text{(iii)}$$

$$O_2\,(l) + x \overset{K_a}{\longleftrightarrow} O_2x \quad \text{(iv)}$$

$$O_2x + HS^- \overset{K_{r1}}{\longleftrightarrow} Sx + OH^- + O^- \quad \text{(v)}$$

$$Sx \longrightarrow S\downarrow + x \quad \text{(vi)}$$

$$O^- + HS^- \overset{K_{r2}}{\longleftrightarrow} S\downarrow + OH^- \quad \text{(vii)}$$

$$H^+ + OH^- \overset{K_e}{\longleftrightarrow} H_2O \quad \text{(viii)}$$

Step (v) was supposed as a control process and step (vi) and (vii) was transient reaction, the solved of H_2S and O_2 fits Henry law in (i) and (ii), the rate of reaction for H_2S are of the form:

$$r_s = -r_A = K_{r1}C_{O_2x}C_{HS^-} + K_{r2}C_{ox}C_{HS^-} = 2K_{r1}C_{O_2x}C_{HS^-} \quad (3)$$

$$r_A = \frac{2K_{r1}K_{e1}C_{xt}K_{HB}K_aP_{O_2}P_{H_2S}}{[H^+](1+K_aK_{HB}P_{O_2})} \times \phi_S \quad (4)$$

where $\phi_S = 1 - C_{sx}/C_{xt}$ is the function of S deposition.

Reaction rate can be express using the rate of S deposited in per gram catalyst as follow:

$$r_A = \frac{1}{M_S}\frac{dW_S}{dt} = \frac{2K_wK_{r1}C_{xt}K_{e1}K_{HA}K_{HB}K_aP_{O_2}P_{H_2S}}{[H^+](1+K_aK_{HB}P_{O_2})} \times \phi_S \quad (5)$$

where K_w is the kinetic rate constant which is dependent on the frame of catalyst (impregnated activated carbon) and contents of H_2O in gas, W_S the adsorbed amount of S per gram adsorbent, M_S the molar quality of S, ϕ_S the function of W_S and saturation S deposited, used a empirical function to replace Eq. (5)

$$\phi_S = (1 - aW_S)^n \quad (6)$$

therefore reaction rate can be expressed as:

$$\frac{dW_S}{dt} = \frac{2M_SK_wK_{r1}(k'/a)K_{e1}K_{HA}K_{HB}K_aP_{O_2}P_{H_2S}}{[H^+](1+K_aK_{HB}P_{O_2})} \times (1 - aW_S)^n \quad (7)$$

or:

$$\frac{dW_S}{dt} = \frac{(k_1k_2/a)P_{O_2}P_{H_2S}}{(1+K_2P_{O_2})} \times (1 - aW_S)^n \quad (8)$$

$$k_1 = \frac{2M_SK_wK_{r1}K_{e1}K_{HA}}{[H^+]} \quad (9)$$

$$k_2 = K_aK_{HB} \quad (10)$$

where $a = k'/C_{xt}$.

For catalytic oxidation reaction of phosphorous, PH_3 was taken as a representation (which is the main container of total phosphorous in tail gas). The reaction process for PH_3 catalytic oxidation reaction (such as R4) may consist of three steps: diffusion from bank of gas to the surface of catalyze (external diffusion), diffusing from surface to the internal surface of catalyze (internal diffusion), PH_3 was adsorbed on the internal surface of catalyze and oxidation reaction took place. The products of oxidation reaction was adsorbed on the surface of catalyze such that the activated center site of catalyze was reduced and finally got saturation. The reaction rate can be expressed:

$$r = -\frac{dC_A}{dt} = \frac{dC_P}{dt} = k^n_{C_A} \quad (11)$$

where C_A represents the concentration of reaction A, C_p the concentration of products, t the reaction time, k means the reaction constant and n is the reaction order.

2.3. Fixed-bed mathematical model of binary gas adsorptive reactor for isothermal dilute systems

According to the analysis above, the mechanism of removing H_2S and PH_3 from yellow phosphorous tail gas over activated carbon impregnated is that catalytic oxidation reaction and physical adsorption took place simultaneously. From an engineering point of view, solving the complete equations of mass, momentum and heat transfer equations requires large computational effort [22,23]. During the past decades, many methods have been employed to model adsorption processes including physic and chemical adsorption in fixed bed [24–29]. Huang et al. [30] proposed a model for gas–solid chemisorption in chemical heat pumps, Wang et al. [31] had studied H_2S catalytic oxidation on impregnated activated. In this work, a new adsorptive reactor model including physical adsorption and chemical reaction occurred simultaneously will be presented to describe the binary gases dynamic behavior for H_2S and PH_3 removing from yellow phosphorous tail gas in fixed bed.

In the case of diluted systems, adsorbed amount of compounds is very small comparing with the total amount of gases entering the column, it is reasonable to suppose that gas density is constant over the entire bed. For this reason, momentum equation can be simplified to obtain a constant profile of velocity not depending on the axial direction. By assuming a quasi-steady, incompressible flow, the two-dimensional mass balance equation for fixed-bed reactor take the form as below:

$$\varepsilon\frac{\partial c_i}{\partial t} = \frac{\partial}{\partial z}\left(D_{zi}\frac{\partial c_i}{\partial z}\right) + \frac{1}{r}\frac{\partial}{\partial r}\left(rD_{ri}\frac{\partial c_i}{\partial r}\right) - u\frac{\partial c_i}{\partial z} - (1-\varepsilon)\rho_c\frac{\partial X_i}{\partial t} - (1-\varepsilon)S_{cat}R_i \quad (12)$$

where ε is bed voidage, D_{zi} is mass diffusivity for gas species i of axial, D_{ri} means mass diffusivity for gas species i of radial, which could be calculated through the method of ref. [32]. c_i is i component concentration in gas, X_i the adsorbed amount i on solid surface, ρ_c the density of solid, S_{cat} the catalytic surface area per unit catalyst volume and R_i is the reaction rate of i.

The boundary conditions for radius are given below:

$$r = \frac{d}{2}, \quad \frac{\partial c_i}{\partial r} = 0 \quad (13)$$

$$r = 0, \quad \frac{\partial c_i}{\partial r} = 0 \quad (14)$$

also condition to axial coordinate are:

$$z = 0, \quad u(c_{\alpha i} - c_i) = -D_{zi}\frac{\partial c_i}{\partial z} \quad (15)$$

$$z = L, \quad \frac{\partial c_i}{\partial z} = 0 \quad (16)$$

the initial condition for mass balance equation is:

$$t = 0, \quad \begin{cases} c_i(0,r,z) = c_{i0} \\ X_i(0,r,z) = X_{i0} \end{cases} \quad 0 \le r \le \frac{D}{2}, \quad 0 \le z \le L \quad (17)$$

adsorption mass transfer rate can be written as:

$$\frac{\partial X_i}{\partial t} = K(c_i - c_i^*) \quad (18)$$

where c_i^* is the adsorption equilibrium concentration for i in gas phase calculated by Eq. (2).

3. Experiment and set up

3.1. Impregnated activated carbon preparation

Two kinds of impregnated activated carbon were prepared. Activated carbon (volume density is 0.67 g/cm^3, BET surface area is 1150 m^2/g, particle size used in experiment is about 2 mm) bought from company was used as the support. Firstly, activated carbon was washed and dried at 100–110 °C for 24 h. For one impregnated activated carbon (named JAC), a known amount of dried activated carbon was stirred in 7% $NaCO_3$ aqueous solution at room temperature for 12 h, and then dried at 110 °C for another 24 h. For another one (named SAC), a known amount of dried activated carbon was impregnated in 5% HCl aqueous solution for 36 h, and then dried at 110 °C for more than 14 h. Before the adsorption experiment, catalysts were activated in situ in a quartz vial adsorber under ultra-pure N_2 at 120 °C at 1 °C/min and the temperature held at that point for 10 h.

3.2. Experimental apparatus and chemical reaction dynamics measurements

3.2.1. Laboratory-scale fixed-bed reactor

An U form quartz adsorber with 10 mm i.d. was employed. Nitrogen (pre-purified grade, Metro welding, 99.995%) was used as the carrier gas and by blending with amount of O_2 and pure H_2S or PH_3, the mixture gas was directed into the adsorber. Analysis of reactor inlet and outlet gas was carried out by a FID spectrometer and a gas chromatography (type 120G). Experimental tail gas was absorbed using Na_2CO_3 and Cu_2SO_4 solution, respectively.

3.2.2. Pilot-plant reactor

A pilot-plant scale experiments of catalytic oxidation were performed in a fixed-bed column with the internal diameter of 0.24 m, height of 2.8 m and gas volume of 50 N m^3/h. The fixed-bed column and yellow phosphorous tail gas were heated by steam indirectly. A schematic flow diagram of catalytic oxidation process is shown in Fig. 1 Experiments were carried out at different temperatures within the range of 20–90 °C. Analysis of the reactor in- and outlet gas was carried out by a FID spectrometer and a gas chromatography (type 120G). The contents of component of yellow phosphorous tail gas used in this experiment described in Table 1.

3.2.3. Chemical kinetics

Chemical kinetics experiment had been studies in a differential reactor with 10 mm i.d. and 500 mm in length stainless steel tube. The concentration of H_2S or PH_3 in mixture gas was regulated by carrier gas (N_2 and amount of O_2) and pre-heated before

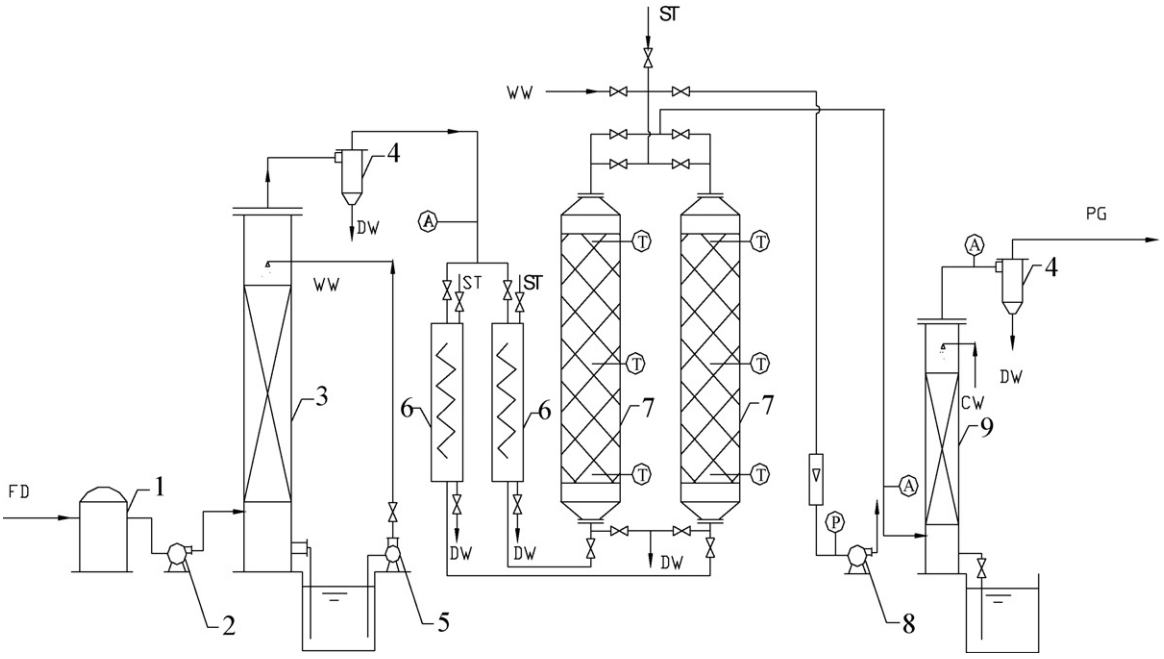

Fig. 1. Flow shame of the apparatus for phosphorous tail gas purification: (1) water seal, (2) vacuum pump, (3) caustic washing tower, (4) mist eliminator, (5) pump, (6) preheated, (7) reactor, (8) induced fan, (9) cooler. T, thermometer; P, pressure gauge; A, sampling.

enter the reactor. Both H_2S and PH_3 flow rates were adjusted by mass-flow meters, respectively. For a reactor being differential is that the conversion of reactants in the bed is extremely small as the change in reactant concentration through the bed. That means, the reactor is considered to be gradient-less, and reaction rate is considered spatially uniform with the bed. Reaction rate is calculated as follow:

$$(-r_A) = \frac{G}{V_R}(C_{Af} - C_{Ao}) \tag{19}$$

where $-r_A$ is the reaction rate for reactant concentration is $C_{Af} + C_{Ao}/2$. In each experiment, 1.0 g catalysts with particle size 1.0 μm were in use. G is the volume rate of reactant.

For H_2S removal, from Eq. (8), the rate of S depositing can be expressed by:

$$\frac{dW_S}{dt} = r_{S0} \times (1 - aW_S)^n \tag{20}$$

where r_{S0} represents the initial rate at $W_S = 0$:

$$r_{S0} = \frac{k_1 k_2 / a P_{O_2} P_{H_2S}}{(1 + K_2 P_{O_2})} \tag{21}$$

Table 1
Contents of component in yellow phosphorous tail gas

Component	Content (%)	Component	Content
CO_2	2.44	N_2	4.29%
O_2	0.5	H_2O	~5%
CO	85.425	H_2S	1050 mg/m^3
H_2	6.47	P[a]	1170 mg/m^3
CH_4	0.425	HF	310 mg/m^3

[a] The total phosphorous containing in the tail gas.

the deposit amount of S is calculated from Eq. (20)

$$W_S = \left\{ \begin{array}{l} \dfrac{[1 - \exp(-a r_{S0} t)]}{a} (n = 1) \\ \dfrac{1}{a}\left\{1 - \dfrac{1}{[1 + (n-1) a r_{S0} t]^{1/n-1}}\right\} (n \neq 1) \end{array} \right\} \tag{22}$$

where n, a and r_{S0} can be simulated through experiments. When $n = 2$, the calculation results shows the best relatively, therefore, for $n = 2$, the Eq. (22) will be:

$$\frac{1}{W_S} = a + \frac{1}{r_{S0}} \frac{1}{t} \tag{23}$$

a and r_{S0} can be calculated from the slop and intercept of line $1/W_S \sim 1/t$. Results of a at different temperature are listed in Table 2. The relationship between a and temperature is fitted with line can be expressed by:

$$a = -1.3219 + 0.1217(T_r - 273.1) \tag{24}$$

Kinetic constants k_1 and k_2 in Eq. (8) could be got through Arrenous equation at different temperature and expressed as

Table 2
Kinetic parameter at different temperature

	T (°C)				
	20	45	60	75	90
a[a]	1.548	3.635	5.734	7.842	9.938
k (1/min × 10^{-3}[b])	3.093	1.508		0.789	0.396

[a] Calculated from Eq. (23).
[b] Kinetic constant for PH_3 come from the slope of lines in Fig. 2.

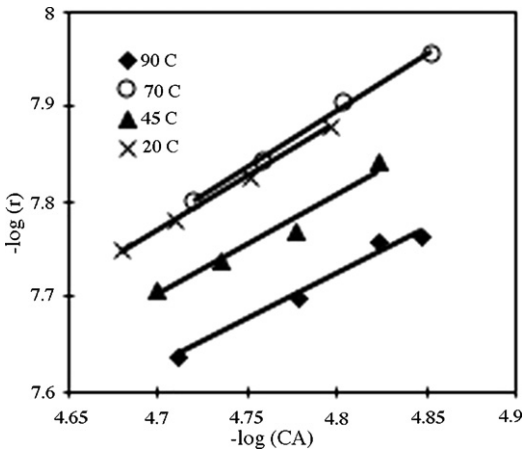

Fig. 2. The relationship between $\log r \sim \log C_A$ at different temperature.

follows:

$$k_1 = 2.271 \times 10^5 \exp\left[\frac{-2698.8}{T_r}\right] \quad (25)$$

$$k_2 = 0.108 \exp\left[\frac{2192}{T_r}\right] \quad (26)$$

For PH_3, from Fig. 2 it can be seen that it was a line relationship between $\log r \sim \log C_A$, that means the reaction order $n = 1$, and kinetic constant can be calculated through the slope and intercept of line $\log r \sim \log C_A$. Results are also listed in Table 2.

4. Numerical solutions

A system of Eq. (12) accompanied by four boundaries (Eqs. (13)–(16)) and one initial condition (Eq. (17)) for two compounds (H_2S and PH_3) are solved simultaneously by finite-difference method. Space grid is chosen to be 0.004 m in radial (Δr) and 0.07 m in axial (Δz), and corresponding time step-size (Δt) being 10 s. Mass transfer process within Δv ($\Delta v = \Delta r \times \Delta z$) during Δt were supposed to be steady. At the same time, the affection of fluid flow distribution in radial were also in computing. The parameters used in calculating were listed in Table 3.

5. Results and discussion

Two impregnated activated carbon, SAC and JAC, were firstly tested in laboratory-scale fixed-bed adsorber at 20 °C. The breakthrough curves of H_2S and PH_3 adsorption on these two kinds of adsorbents are shown in Figs. 3 and 4. It is indicated that the adsorption capacity of SAC was higher for PH_3 than for H_2S, whereas the adsorption capacity of JAC was better for H_2S than for PH_3. Breakthrough time is 2000 min for H_2S JAC and 500 min for PH_3 on SAC. When adsorbents were used oppositely, H_2S was adsorbed on SAC and PH_3 was adsorbed on JAC, breakthrough time is only approximately 10 min for both two adsorbates. It is clear that there will not get desirous results for purification real yellow phosphorous tail gas only using one

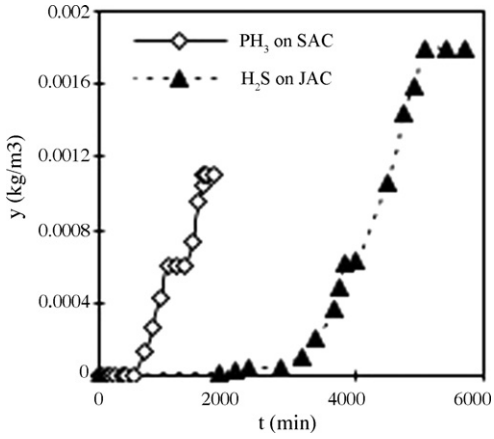

Fig. 3. Breakthrough curve of H_2S adsorption on JAC and PH_3 adsorption on SAC.

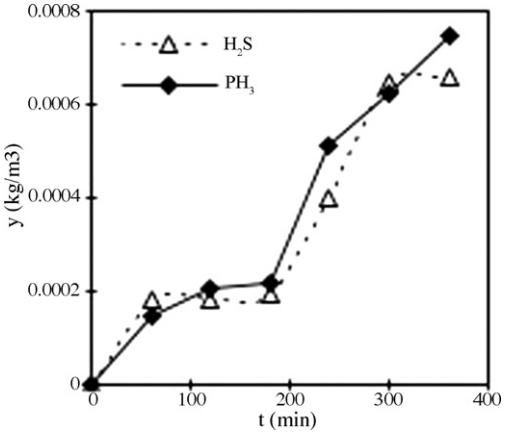

Fig. 4. Breakthrough curve of H_2S adsorption on SAC and PH_3 adsorption on JAC.

of these impregnated activated carbon as an adsorbent. Fig. 5 shows the breakthrough curves for H_2S and PH_3 on a mixture adsorbent (half of SAC and half of JAC) at room temperature. It is clear that the mixture adsorbent has better adsorption capacity for both H_2S and PH_3, although the adsorption capacity for these two compounds are less than that one adsorbent for pure component shown in Fig. 3, it will be useful for P and S

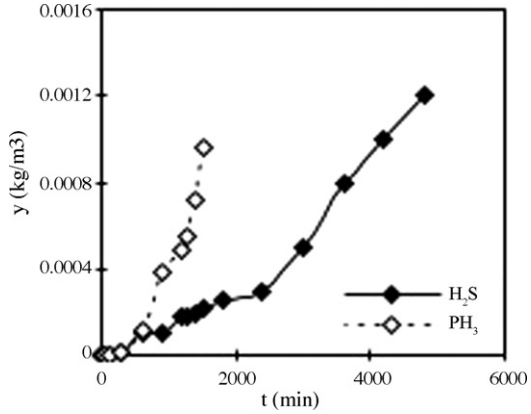

Fig. 5. Breakthrough curve of H_2S and PH_3 adsorption on mixture sorbent at 20 °C.

Table 3
Simulation parameters for isotherms and model calculation

ε	ρ_c (kg/m^3)	K (m^3 kg s^{-1})	z (m)	Δz (m)	d (m)	Δr (m)	X_0 (kg kg^{-1})	Δt (s)
0.37	670	0.028	2.8	0.07	0.24	0.004	1×10^{-8}	10

	Q_m	b
H_2S	0.2789	665.84
PH_3	0.00134	1636.31

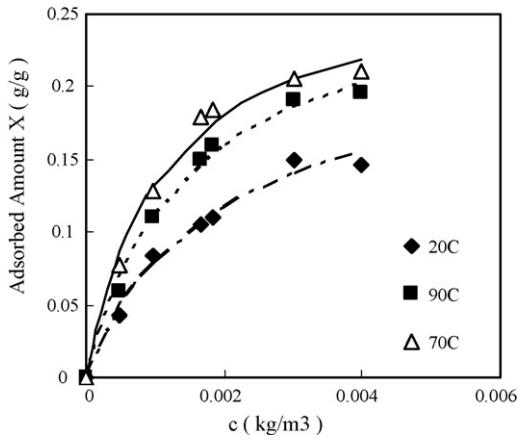

Fig. 6. Adsorption isotherms of H_2S on impregnated activated carbon, at different temperature, solid or dash line is fitted with Langmuir model.

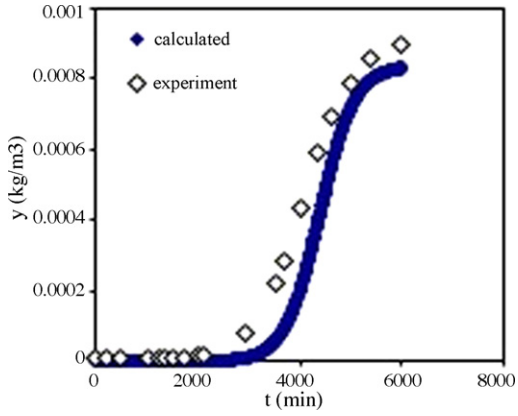

Fig. 8. Comparing breakthrough curve of experiment in pilot-plant scale reactor using model gas (N_2 and amount of O_2) with model predicted for H_2S adsorption at 70 °C, space velocity 800 h^{-1}.

removal simultaneously for real yellow phosphorous tail gas in industry.

The first step in the characterization of a material for a specific adsorption separation process is to measure the adsorption equilibrium of pure components. Adsorption equilibrium of pure H_2S and PH_3 at different temperature are shown in Figs. 6 and 7. Langmuir isotherm model was used to fit and analyze the data of pure gases used in this work. Fitted parameters used in Eq. (2) are listed in Table 3. It is noticed that the adsorbent has better adsorption capacity for both H_2S and PH_3 at 70 °C. Therefore, reaction temperature at pilot-scale was taken at 70 °C.

Fig. 8 compares the breakthrough curve between calculation by modeling and measured data in pilot-plant scale reactor using model gas (N_2 and amount of O_2) for H_2S removal. Model prediction is good agreement with experimental.

Fig. 9 shows the breakthrough curve of PH_3 come from model predicting and experiment in pilot-plant reactor for real yellow phosphorous tail gas. Model predicting is agreement with experiment. The error between predicted and experiment may contribute from the affect of other low concentration compounds contained in tail gas listed in Table 1. At this time, H_2S in the out-

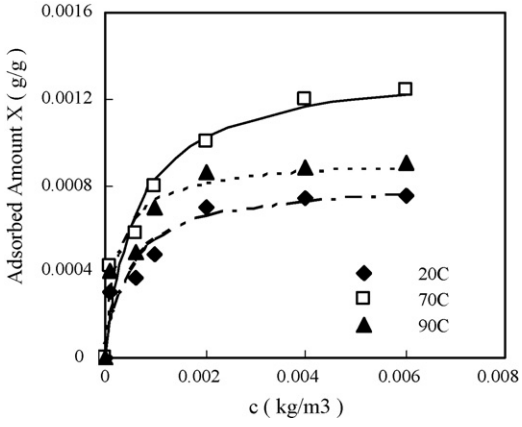

Fig. 7. Adsorption isotherms of PH_3 on impregnated activated carbon, at different temperature, solid or dash line is fitted with Langmuir model.

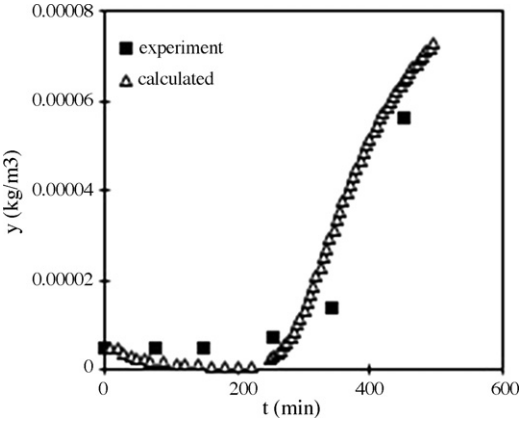

Fig. 9. Comparing breakthrough curve of experiment in pilot-plant reactor for real yellow phosphorous tail gas with model predicted for PH3 adsorption at 70 °C, space velocity 400 h^{-1}.

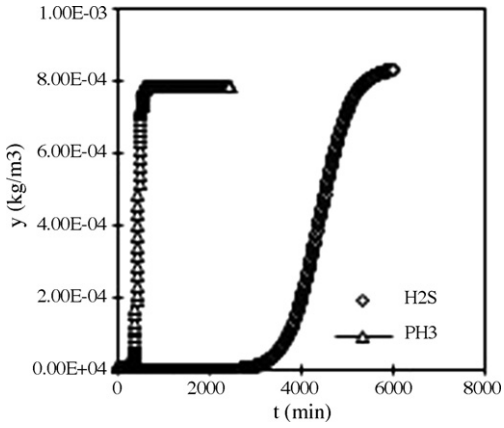

Fig. 10. Comparing breakthrough curve of H_2S and PH_3 on pilot-plant reactor by model prediction at 70 °C 800 h^{-1}.

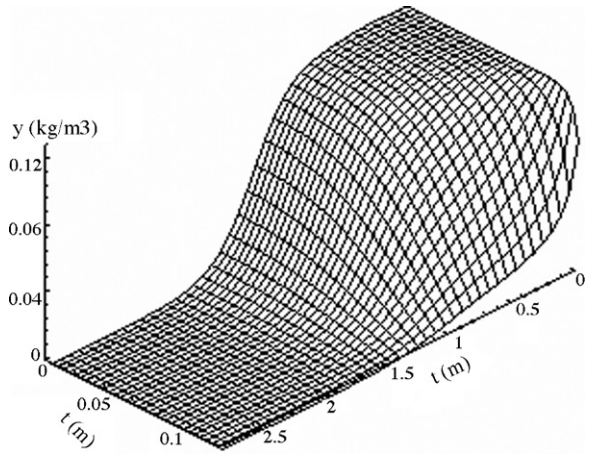

Fig. 12. Concentration distribution of PH_3 in gas phase in the reactor alone radial and axial at 300 min and 600 h^{-1} space velocity by the model prediction.

let of reactor cannot be tested, that means during the pilot-plant process reaction time is mainly depended on the breakthrough time of PH_3.

Fig. 10 shows the outlet concentration varieties with time for H_2S and PH_3 by model calculated in pilot-plant reactor. Comparing with Fig. 5, it is indicated that due to the catalytic oxidation reaction taking place breakthrough time difference between H_2S and PH_3 increased, which means at this reaction condition the selective of catalyze is more higher for H_2S than for PH_3. Breakthrough time of H_2S is nearly 3000 min at 800 h^{-1} space velocity, it is almost 10 times than that of PH_3. Figs. 8 and 9 also indicated the same results.

Figs. 11 and 12 show the concentration distribution of H_2S and PH_3 in gas phase in the reactor alone radial and axial at 300 min and 600 h^{-1} space velocity by model prediction. It is clear that the concentration of both gas compounds decreased from centre to the wall in the radius. Figs. 13 and 14 show the concentration distribution in the middle of reactor in axial at different time by model calculation. From the model prediction, it is easy to know the detail concentration distribution of component in reactor. It is useful for designing of a real yellow phosphorous tail gas purification plant.

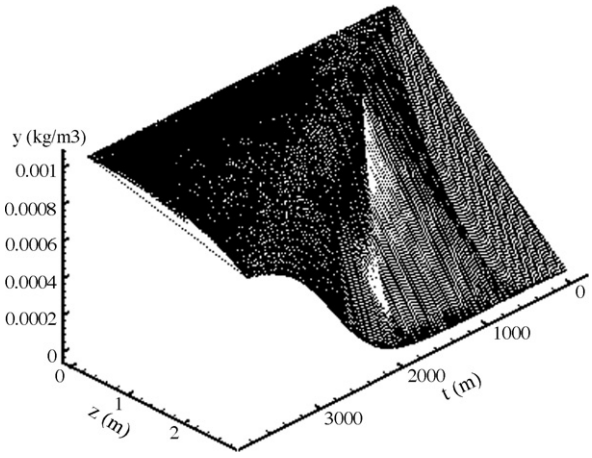

Fig. 13. Concentration distribution of H_2S in the middle of reactor in axial at different time by model calculation.

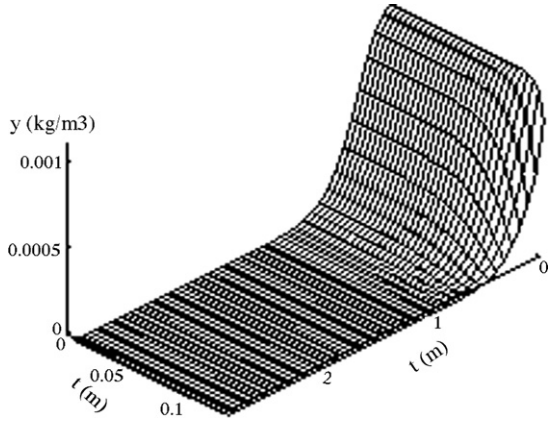

Fig. 11. Concentration distribution of H_2S in gas phase in the reactor alone radial and axial at 300 min and 600 h^{-1} space velocity by the model prediction.

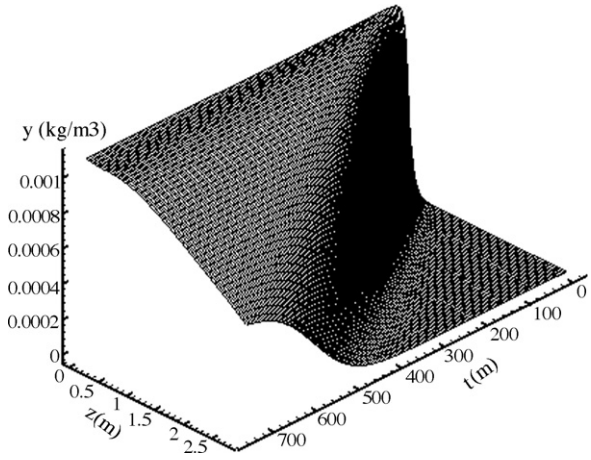

Fig. 14. Concentration distribution of PH_3 in the middle of reactor in axial at different time by model calculation.

6. Conclusion

Two kinds of impregnated activated carbon were prepared to remove H_2S and PH_3 in yellow phosphorous tail gas. The removal of H_2S and PH_3 through a impregnated activated carbon fixed bed can be considered as an adsorptive reaction process which involves two independent processes: physical adsorption and catalytic oxidation reaction. The performances of laboratory-scale and pilot-plant fixed bed have been assessed for both impregnated activated carbon. A mixture catalyze was used to remove both S and P compounds simultaneously in real yellow phosphorous tail gas. Adsorption kinetic and reaction kinetic of this process were studied over the mixture impregnated activated carbon. After purification through the catalyze bed, the concentration of H_2S and PH_3 in tail gas would be $PH_3 < 5\ mg/m^3$, $H_2S < 5\ mg/m^3$, which can be used as a source for further products.

A two-dimensional non-steady binary mixture gases adsorption-reaction mathematical model were developed to simulated the pilot-plant reactor for removing H_2S and PH_3 simultaneously. On the whole, the model predictions match the experimental pilot-plant data for both compounds. From the prediction of model, the detail concentration distribution of compounds in gas or solid phase can be observed. It is thus a very useful tool to support the proper design of industrial yellow phosphorous tail gas purification unit.

Acknowledgment

Financial support for this project was provided by National Natural Science Foundation of China (NNSF), which is greatly acknowledged.

References

[1] P. Ning, Y.Ch. Xie, H.H. Yi, Study on a four-bed PSA process for the manufacture of pure CO, in: Proceedings of Seventh International Conference of Fundamentals of Adsorption, Nagasaki, Japan, 2001, pp. 613–617.
[2] Y.-Ch. Xie, J.P. Zhang, Adsorption isotherms for PU1 and its application in industry, in: Proceedings of Seventh International Conference of Fundamentals of Adsorption, Nagasaki, Japan, 2001, pp. 561–563.
[3] B.S. Shakirv, St. Prom, Pretreatment and purification of yellow phosphoric tail gas, Moscow, vol. 148, 1993, pp. 3–4.
[4] K.T. Zhantasov, Impurities remove from yellow phosphoric tail gas, Vestn. Minist. Nauki-Akak. Nauk Res. Kaz. 5 (1997) 52.
[5] P.R. Westmoreland, D.P. Harrison, Evaluation of candidate solids for high temperature desulfurization of low BTU gases, Environ. Sci. Technol. 10 (1976) 659–663.
[6] L.A. Fenouil, G.P. Towler, S. Lynn, Removal of H_2S from coal gas using limestone: kinetic consideration, Ind. Eng. Chem. Res. 33 (2) (1994) 265–272.
[7] L.A. Fenouil, S. Lynn, Study of calcium-based sorbents for high-temperature H_2S removal. 2. Kinetic of H_2S sorption by calcined limestone, Ind. Eng. Chem. Res. 34 (7) (1995) 2334–2342.
[8] S.S. Chauk, R. Agnihotri, R.A. Jadhav, Kinetic of high-pressure removal of hydrogen sulfide using calcium oxide powder, Am. Ind. Chem. Eng. J. 46 (6) (2000) 1157–1167.
[9] F. Garcia-Labiano, A. Abad, L.F. De Diego, Calcination of calcium-based sorbents at pressure in a board range of CO_2 concentrations, Chem. Eng. Sci. 57 (13) (2002) 2381–2393.
[10] J. Abbasian, R.B. Slimane, A regenerable copper-based sorbent for H_2S removal from coal gases, Ind. Eng. Chem. Res. 37 (1998) 2775–2782.
[11] E. Suvar, H. Radamson, J.V. Grahn, Phosphorus profile control in low-temperature silicon epitaxy by reduced pressure chemical vapor deposition, Mater. Sci. Eng. B 89 (2002) 314–323.
[12] Y. Sun, D.C. Law, R.F. Hicks, Kinetics of phosphine adsorption and phosphorus desorption from gallium and indium phosphide (0 0 1), Surf. Sci. 540 (2003) 12–22.
[13] A. Sirkecioglu, Y. Altav, A.S. Erdem, Adsorption of H_2S and SO_2 on Bigadiç Clinoptilolite, Sep. Sci. Technol. 30 (1995) 2747–2756.
[14] L. Wang, B. Cao, S.D. Wang, Q. Yuan, H_2S catalytic oxidation on impregnated activated carbon: experiment and modeling, Chem. Eng. J. 118 (2006) 133–139.
[15] R. Wang, Investigation a new liquid redox method for removal H_2S and sulfur recovery with heteropoly compound, Sep. Purif. Technol. 31 (2003) 111–121.
[16] E.J. Sasaoka, Catalytic activity of ZnS formed from desulfurizetion sorbent ZnO for conversion of COS to H_2S, Ind. Eng. Chem. Res. 34 (1995) 1102–1109.
[17] M. Echard, L. Leglise, H2S adsorption on a sulfided $CoMo/Al_2O_3$ catalyst under flow and pressure conditions: a thermodynamic and modelization study, Thermochim. Acta 379 (2001) 241–254.
[18] R.C. Bansal, J.B. Donnet, F. Stoeckli, Activated Carbon, Dekker, New York, 1988.
[19] Y.C. Chung, K.L. Ho, C.P. Tseng, Treatment of high H_2S concentrations by chemical adsorption and biological oxidation process, Environ. Eng. Sci. 23 (6) (2006) 942–953.
[20] A.N. Kaliva, J.W. Smith, Oxidization of low concentration of hydrogen sulfide by air on a fixed activated carbon, Can. J. Chem. Eng. 61 (1983) 208–212.
[21] R.T. Yang, Gas Separation by Adsorption Process, Butterworths, London, 1987.
[22] S. Suwanprasop, A. Eftaxias, F. Stuber, I. Polaert, C.J. Lebigue, H. Delmas, Scale-up and modeling of fixed-bed reactors for catalytic phenol oxidation over adsorptive active carbon, Ind. Eng. Chem. Res. 44 (2005) 9513–9523.
[23] N. Yasyerli, T. Dogu, G. Dogu, I. Ar, Deactivation model for textural effects on kinetics of gas–solid noncatalytic reactions—char gasification with CO_2, Chem. Eng. Sci. 51 (1996) 2523–2533.
[24] J.T. Konttinen, C.A.P. Zevenhoven, M.M. Hupa, Hot gas desulfurization with zinc titanate sorbents in a fluidized bed 2. Reactor model, Ind. Eng. Chem. Res. 36 (1997) 2340–2349.
[25] J.T. Konttinen, C.A.P. Zevenhoven, M.M. Hupa, Determination of sorbent particle conversion rate model parameters, Ind. Eng. Chem. Res. 36 (1997) 2336–2345.
[26] H.J. Bart, P. Ning, R. Germerdonk, Two-dimensional non-isothermal model for toluene adsorprion in a fixed bed adsorber, Chem. Eng. Process. 35 (1996) 57–63.
[27] H.J. Bart, Numerical simulation of toluene adsorption on activated carbon in a technical column in low concentration range, Chem. Eng. Technol. 19 (4) (1996) 296–303.
[28] H.P. Zhang, D.Y. Cheng, Mathematical model for a fixed bed adsorptive reactor, Carbon 38 (2000) 877–880.
[29] J.J. Gu, H.J. Bart, Heat and mass transfer in steam desorption of an activated carbon adsorber, Inter. Commun. Heat Mass Trans. 32 (2005) 296–304.
[30] H.J. Huang, G.B. Wu, J. Yang, Y.C. Dai, Modeling of gas–solid chemisorption in chemical heat pumps, Sep. Purif. Technol. 34 (2004) 191–200.
[31] L. Wang, B. Cao, S.D. Wang, Q. Yuan, H_2S catalytic oxidation on impregnated activated carbon: experiment and modelling, Chem. Eng. J. 118 (2006) 133–139.
[32] P. Ning, Numerische simulation des sorptionsverhaltnisses der schadstoffe in kleintechnischen aktivkohlekolonnen im umweltrelevanten konzentrationsbereich unter berucksichtigung von warmeeffekten und maldistribution, Shaker Verlag, Aachen, 1996.